LipidTOX: A fatty acid-based index efficient for ecotoxicological studies with marine model diatoms exposed to legacy and emerging contaminants

Bernardo Duarte [a,b,*], Eduardo Feijão [a], Marco Franzitta [a], Irina A. Duarte [a], Ricardo Cruz de Carvalho [a,c], Maria Teresa Cabrita [d], João Carlos Marques [e], Isabel Caçador [a,b], Vanessa Fonseca [a,f], Ana Rita Matos [b,g]

[a] MARE—Marine and Environmental Sciences Centre, ARNET–Aquatic Research Infrastructure Network Associated Laboratory, Faculty of Sciences of the University of Lisbon, Campo Grande, 1749-016 Lisboa, Portugal
[b] Departamento de Biologia Vegetal da Faculdade de Ciências da Universidade de Lisboa, Campo Grande, 1749-016 Lisboa, Portugal
[c] cE3c – Centre for Ecology, Evolution and Environmental Changes, Faculdade de Ciências, University of Lisbon, 1749-016, Portugal
[d] Centro de Estudos Geográficos (CEG), Instituto de Geografia e Ordenamento do Território (IGOT), University of Lisbon, Rua Branca Edmée Marques, 1600-276 Lisbon, Portugal
[e] University of Coimbra, MARE—Marine and Environmental Sciences Centre, ARNET–Aquatic Research Infrastructure Network Associated Laboratory, Department of Life Sciences, 3000-456 Coimbra, Portugal
[f] Departamento de Biologia Animal da Faculdade de Ciências da Universidade de Lisboa, Campo Grande, 1749-016 Lisboa, Portugal
[g] Biosystems and Applied Sciences Institute, Faculdade de Ciências da Universidade de Lisboa, Campo Grande, 1749-016 Lisbon, Portugal

ARTICLE INFO

ABSTRACT

Contaminants, when present above certain thresholds, can induce physiological constraints to organisms, namely diatoms, a model group representative of marine phytoplankton, triggering feedback mechanisms, such as changes in cell's fatty acid profiles, that can be used as biomarkers towards xenobiotic exposure. Having this in mind and considering the ecological relevance of diatom fatty acid profiles as well as their recognized potential as biomarkers of contaminant exposure, the present work aims to develop and test the accuracy of an integrative multi-biomarker response index based on the fatty acid profiles of marine diatoms (using *Phaeodactylum tricornutum* as model diatom) exposed to several emerging contaminants.

In terms of the impacts at the individual fatty acid level, it was possible to observe changes transversal to different contaminants, such as the reduction of C14:0 and C16:0 fatty acids, with increasing xenobiotic concentration, as observed, for example, under propranolol and fluoxetine exposure. Enhancement of C16:2n-7 and C16:3n-4 concentrations as well as complete disruption of the basal fatty acid profile was observed in diatoms exposed to copper nanoparticles. These individual diverse and intrinsically connected alterations in fatty acid concentrations depended on the type and dose of the xenobiotic applied, highlighting the need to address these profiles as a whole. The evaluation of the diatom cells' fatty acids using a multivariate approach revealed a high degree of sensitivity of these biochemical traits to disclose the type of xenobiotic applied to the diatoms, as well as the exogenous concentration used. These biochemical profiles were later incorporated into a unifying numerical index (LipidTOX) using an integrated biomarker response approach. The LipidTOX index showed strong correlations with both the exogenous xenobiotic concentration applied as well as with the growth features assessed for the exposed cultures, revealing a very high efficiency in translating growth impairments imposed by each of the xenobiotics tested at the different test concentrations. The LipidTOX index proved to be an efficient tool for ecotoxicological assays with marine model diatoms and evidenced a high degree of reliability for classifying the exposure of the cells to emerging contaminants. The results and benefits of the LipidTOX index application can be easily communicated to non-expert audiences such as stakeholders, policymakers and environmental managers so that this approach can be used in future toxicological evaluations of the impacts of classical and emerging xenobiotics in marine primary producers.

* Corresponding author.
  E-mail address: baduarte@fc.ul.pt (B. Duarte).

1. Introduction

The unprecedented human development has unleashed an unparalleled development of new chemical solutions to everyday challenges (CAS, 2011). Coastal areas include many of the world's large cities and are thus associated with large and growing human settlements, implying significant unabated pressures on the coastal and marine realms (von Glasow et al., 2013). Due to the insufficient number and lack of efficiency of wastewater treatment plants (WWTPs) and to unregulated and/or illegal waste disposal, new chemical compounds are being continuously released into the coastal systems (Alygizakis et al., 2016; aus der Beek et al., 2016; Reis-Santos et al., 2018). Although this is more evident in the vicinity of large metropolitan areas (Alygizakis et al., 2016; Aminot et al., 2018; Fonseca et al., 2020; Reis-Santos et al., 2018), the high persistence of these compounds, led to their detection even in remote areas without permanent human activity (Duarte et al., 2021d). The presence of these compounds in marine ecosystems compels the authorities to undertake environmental risk assessment (ERA) actions to disclose the potential impacts of these emerging compounds in marine organisms (Fonseca et al., 2021). For this purpose, there is also a rising need to perform ecotoxicological trials to produce relevant data to feed into these ERA models, enabling appropriate management and stakeholders' entities to perform an accurate environmental assessment. Emerging compounds such as pharmaceuticals, personal care products, biocides and nanomaterials impose serious threats to marine life, with recognized effects observed under current environmental concentrations (Brausch et al., 2012; Duarte et al., 2020b; Fonseca et al., 2021; Franzitta et al., 2020; Lopes et al., 2020; Pires et al., 2021; Roma et al., 2020).

The aforementioned impacts are felt throughout the trophic web, resulting in the most diverse array of effects according to the organisms affected (Brausch et al., 2012; Lopes et al., 2020; Pires et al., 2021; Roma et al., 2020). However, these effects are even more critical when they occur at the basis of the trophic chains, at the primary producers' level, directly and indirectly imposing serious ecosystem shifts. Coastal ecosystems can be directly impacted by the decline in abundance and function impairment of the phytoplanktonic communities, and indirectly by disturbance of energy fluxes (in the form of carbohydrates, fatty acids and other essential nutrients) and oxygen provided by phytoplankton to the upper trophic levels (Cabrita et al., 2016; Duarte et al., 2020b; Feijão et al., 2020a). Diatoms compose the majority of the estuarine and marine phytoplankton communities (Cloern, 2018; Gameiro et al., 2007), and also respond rapidly to changing environmental conditions (Cabrita et al., 2018), thus arising as relevant organisms to address the impacts of emerging contaminants in coastal systems and specifically in the phytoplanktonic compartment. One of the most relevant compounds that phytoplankton make available to the rest of the trophic web are fatty acids, namely long-chain polyunsaturated fatty acids (LC-PUFA) (Jónasdóttir, 2019). Fatty acids have been proved to be a suitable source of biomarkers towards environmental stresses (Duarte et al., 2018c; Duarte et al., 2019a; Duarte et al., 2020d; Feijão et al., 2020c) including contaminant exposure, especially in marine diatoms (Cruz de Carvalho et al., 2020c; B. Duarte et al., 2020b; Feijão et al., 2020a; Franzitta et al., 2020; Silva et al., 2020a). However, fatty acid profiles constitute a dataset composed of several quantitative variables that are not of easy understanding by a non-expert audience. This way and similarly to what has been previously proposed for other biomarker sets such as photochemical datasets (Cruz de Carvalho et al., 2020a) and classical enzymatic biomarkers (Pires et al., 2021), the gathering of these variables into unifying indexes has previously provided consistent and reliable results, in translating the stress condition to which the organisms are subjected to. This approach involving fatty acid profiles was already undertaken to index development for macroalgae (Duarte et al., 2021a) and higher plants (Duarte et al., 2018a), but not yet for marine diatoms.

Due to its cosmopolitan distribution (Cabrita et al., 2017), fully sequenced genome (Bowler et al., 2008), and role as biomonitor species able to reflect early signs of stress, *Phaeodactylum tricornutum* Bohlin (Bacillariophyceae) has gained a significant role in stress biology and ecotoxicological studies. Several studies have used this species as model to study the effects of a wide array of contaminants namely heavy metals (Cabrita et al., 2017; Cid et al., 1995), metal nanoparticles (Franzitta et al., 2020; Li et al., 2017; Wang et al., 2016), polycyclic aromatic hydrocarbons (Wang et al., 2008; Wang and Zheng, 2008), biocides (Du et al., 2019), surfactants (Pavlić et al., 2005), ionic liquids (Chen et al., 2019) and pharmaceutical residues (Duarte et al., 2021c), among several others. Thus it is a highly relevant species for ecotoxicology purposes and the development of indexes based in its physiological response to contaminants is of added value for ecotoxicological studies (Duarte et al., 2021c; Pires et al., 2021; Rodrigues et al., 2021).

In this context and considering the ecological relevance of diatom fatty acid profiles as well as their recognized potential as biomarkers of contaminant exposure, the present work aims to develop and test the accuracy of an integrative multi-biomarker response index based on the fatty acid profile of marine diatoms under the exposure to several emerging contaminants. Beyond the undeniable ecotoxicological and physiological applications in future research studies, this index would also provide a tool for communication of the relevant effects of contaminants in marine diatoms, as model organisms, and their fatty acids as biomarkers, to stakeholders, managers, decision, and policymakers in ecotoxicological, environmental risk assessment and biomonitoring studies.

2. Materials and methods

2.1. Diatom exposure trials

Data regarding growth and biomarker activity/concentration were collected from previously published works (Cruz de Carvalho et al., 2020c; B. Duarte et al., 2020b; Feijão et al., 2020b; Silva et al., 2020b). *Phaeodactylum tricornutum* Bohlin (Bacillariophyceae; strain IO 108–01, Instituto Português do Mar e da Atmosfera IPMA)) axenic cell cultures (maintained under asexual reproduction conditions) were placed to grow in f/2 medium (Guillard and Ryther, 1962), under constant aeration in a phytoclimatic chamber, at 18 °C, programmed with a 14/10 h day/night photoperiod (RGB 1:1:1, maximum PAR 80 μmol photons m^{-2} s^{-1}), a sinusoidal function to mimic sunrise and sunset, and light intensity equal to noon, set to replicate a natural light environment (Feijão et al., 2018). Exposure trials were conducted according to the Organization for Economic Cooperation and Development (OECD) recommendations for algae assays (OECD, 2011), with minor adaptations, and as described in previous studies (Cruz de Carvalho et al., 2020c; Duarte et al., 2020b; Feijão et al., 2020b; Silva et al., 2020b). Briefly, cultures were exposed to compounds and target concentrations for 48 h. Target concentrations were selected aiming to cover a concentration gradient reflecting, not only the detected environmental concentrations found in the literature but also concentrations known to have significant biological effects in *P. tricornutum* (Claessens et al., 2013; Franzellitti et al., 2015) (Table 1). Bezafibrate, fluoxetine, propranolol, ibuprofen, glyphosate, SDS and triclosan were supplied to the cultures in its pure form. The ionic Cu form was CuSO$_4$, whilst Cu NPs were purchased as CuO nanoparticles with a particle size < 50 nm and a surface area of 29 m^2 g^{-1} (Sigma-Aldrich, product reference 544868). Data regarding Cu nanoparticles electrochemical behaviour and dispersion in the present culture conditions can be found in Franzitta et al. (2020). Selected contaminants were based in its presence and abundance in marine transitional systems from previous works (Claessens et al., 2013; Franzellitti et al., 2015; Reis-Santos et al., 2018). In order to evaluate the potential effects of nanoparticle toxicity, Cu NPs were selected due to its widespread use in several applications from agriculture, to cosmetics and biocides and thus potential increase in the aquatic environment (Liu et al., 2018).

Table 1

Tested xenobiotic, respective classes and applied concentrations.

Xenobiotic	Classification	Concentration
Bezafibrate	Pharmaceutical compound Lipid regulator	0 µg L^{-1}
		3 µg L^{-1}
		6 µg L^{-1}
		30 µg L^{-1}
		60 µg L^{-1}
		300 µg L^{-1}
Fluoxetine	Pharmaceutical compound Antidepressant	0 µg L^{-1}
		0.3 µg L^{-1}
		0.6 µg L^{-1}
		20 µg L^{-1}
		40 µg L^{-1}
		80 µg L^{-1}
Propranolol	Pharmaceutical compound β-blocker	0 µg L^{-1}
		0.3 µg L^{-1}
		8 µg L^{-1}
		80 µg L^{-1}
		150 µg L^{-1}
		300 µg L^{-1}
Ibuprofen	Pharmaceutical compoundNon-steroidal anti-inflammatory drug (NSAID)	0 µg L^{-1}
		0.8 µg L^{-1}
		3 µg L^{-1}
		40 µg L^{-1}
		100 µg L^{-1}
		300 µg L^{-1}
Glyphosate	Pesticide	0 µg L^{-1}
		10 µg L^{-1}
		50 µg L^{-1}
		100 µg L^{-1}
		250 µg L^{-1}
		500 µg L^{-1}
SDS	Personal Care Product Anionic Surfactant Detergent	0 mg L^{-1}
		0.1 mg L^{-1}
		1 mg L^{-1}
		3 mg L^{-1}
		10 mg L^{-1}
Triclosan	Personal Care Product Antimicrobial	0 µg L^{-1}
		0.1 µg L^{-1}
		1 µg L^{-1}
		10 µg L^{-1}
		50 µg L^{-1}
		100 µg L^{-1}
Dissolved Cu	Trace element Soluble salt form	0 µg L^{-1}
		1 µg L^{-1}
		5 µg L^{-1}
		10 µg L^{-1}
Cu NP	Trace element Nanoparticle form	0 µg L^{-1}
		1 µg L^{-1}
		5 µg L^{-1}
		10 µg L^{-1}

2.2. Fatty acid analysis

Diatom pellets were submitted to direct transesterification with daily prepared methanol sulfuric acid (97.5:2.5, v/v) at 70 °C for 60 min (Matos et al., 2007). Subsequently, fatty acids methyl esters (FAMEs) were recovered using petroleum ether and the solvent evaporated under an N$_2$ flow in a dry bath at 30 °C (Duarte et al., 2018b). FAMEs were resuspended in hexane and 1 µL was injected in a gas chromatograph (Varian 430-GC gas chromatograph, Middelburg, The Netherlands), equipped with a hydrogen flame ionization detector set at 300 °C. The temperature of the injector was set to 270 °C, with a split ratio of 50. The fused-silica capillary column (50 m × 0.25 mm; WCOT Fused Silica, CP-Sil 88 for FAME; Varian, Middelburg, The Netherlands) was maintained at a constant N$_2$ flow of 2.0 mL min^{-1} and the oven set at 190 °C. Fatty acid identification was achieved by comparison of retention times with standards (Sigma-Aldrich, USA), and chromatograms were analysed by the peak surface method, using Galaxy software. The internal standard used was pentadecanoic acid (C15:0).

2.3. LipidTOX integrated biomarker response index

An integrated biomarker response (IBR) index approach was attained for the LipidTOX index development and was calculated for each tested compound according to (Beliaeff and Burgeot, 2002a), posteriorly adapted (Broeg and Lehtonen, 2006). Briefly, it was calculated by summing up triangular star plot areas calculated for every two neighbouring variables. To calculate IBR integrating all fatty acids, data of each fatty acid were standardized to obtain Y as:

$$Y = \frac{X - m}{s}$$

where X is the value for each fatty acid replicate within a given concentration, m is the general mean of all data (including concentrations) regarding a given fatty acid, and s is the standard deviation of the biomarker data for a given treatment/concentration. Then, Z was calculated using Z = -Y or Z = Y, in the case of a biological effect corresponding respectively to inhibition or stimulation and it was determined using the slope of the fatty acid concentration towards the applied exogenous concentration. Positive slopes corresponded to stimulation, while negative slopes corresponded to an inhibition. Regarding the biological effect, fatty acids can either increase or decrease depending on the type and concentration of the compound exposure, but they can also vary among organisms.

Subsequently, the score (S) was calculated as.

$$S = Z + |Min|$$

where, S ≥ 0 and |Min| is the absolute value for the minimum value for all calculated Y for a given fatty acid at all the made measurements (again all concentrations considered). Star plots were then used to display score results (S) and to calculate the LipidTOX index as:

$$LipidTOX = \sum_{t=15}^{n} A_i$$

A$_i$ is the area between two consecutive clockwise scores in each star plot:

$$A_i = \frac{S_i}{2}\sin\beta(S_i\cos\beta + S_{i+1}\sin\beta)$$

$$\beta = \tan^{-1}\frac{S_{i+1}\sin\alpha}{S_i - S_{i+1}\cos\alpha}$$

where S$_i$ and S$_{i+1}$ are two consecutive clockwise scores of a given star plot; n the number of biomarkers (fatty acids) used and α:

$$\alpha = \frac{2\pi}{n}$$

A normalized LipidTOX (n-LipidTOX) version was also calculated, where the index deviation towards the control was evaluated:

$$n - LipidTOX = LipidTOX_{\left[Xenobiotic_{i,d}\right]_j}^{Xenobiotic_i} - \overline{LipidTOX_{Control}}$$

where the value of the LipidTOX index correspondent to a replicate *j* of the culture exposed to a concentration *d* of the xenobiotic *i* is subtracted to the average value of the LipidTOX index for the control condition.

2.4. Statistical analysis

Permutational multivariate analysis of variance (PERMANOVA) analysis was carried out using Primer 6 software (version 6.1.13, Plymouth, UK) (Clarke and Gorley, 2006). Canonical analysis of principle (CAP) coordinates, using Euclidean distances, were performed to plot in a canonical space the dissimilarities regarding fatty acids relative abundances while performing a cross-validation step and determining the allocation efficiency into the different sample groups (xenobiotic

treatments). This multivariate methodology is unaffected by heterogeneous data and frequently used to compare different sample assemblies using the inherent features of each assembly (metabolic traits) (Cabrita et al., 2018; Duarte et al., 2018; Duarte et al., 2019b, 2017). Heatmaps were constructed using *ggplot2* package (Wickham, 2009) in R-Studio Version 1.4.1717. Spearman correlation coefficients and statistical significance between the fatty acid traits, index, exogenous concentration, and growth traits values were computed using the *corrplot* package (Taiyun, 2021) in R-Studio Version 1.4.1717. Non-parametric Kruskal-Wallis with Bonferroni post-hoc were performed using the *agricolae* package (De Mendiburu and Simon, 2015) in R-Studio Version 1.4.1717. Violin plots with probability density of the data at different values smoothed by a kernel density estimator were computed and plotted using the *ggplot2* package (Wickham, 2009) in R-Studio Version 1.4.1717.

3. Results

3.1. Diatom growth rates and inhibition

Data regarding the specific growth rate and growth inhibition effects of the evaluated xenobiotics on the marine diatom *P. tricornutum* were obtained from previous studies and are presented in Table 2. It was found that the different xenobiotics have very different impacts on the diatom growth, ranging from enhanced cell growth in the cultures exposed to bezafibrate, to severe growth inhibitions and decreased growth rates in the cultures subjected to fluoxetine and glyphosate. This data was previously discussed from the metabolic and biochemical point of view in the references cited in Table 2 and will be later discussed in the present work as growth descriptors of the ecotoxicological status of the cultures.

3.2. Fatty acid concentration under different xenobiotic exposures

From an ecotoxicological point, these results will be analysed by comparing the results attained in the exposed cultures towards the control condition. The most abundant fatty acids present in *Phaeodactylum tricornutum* are C16:0, C16:1n-7 and C20:5n-3 and with some exceptions this was not altered in cells exposed xenobiotics (Fig. 1). The exceptions correspond to the cells exposed to bezafibrate (Fig. 1A) and Cu (Fig. 1H and 1I). Bezafibrate induced a shift in the abundance of the C20:5n-3 towards an increased abundance in the C20:4n-6. As for the cells exposed to Cu, a reduction in the C20:5n-3 with a simultaneous increase in the concentration of C16:3n-4 were observed. In general, exposure to contaminants resulted in significant alterations of the diatoms fatty acid profiles when compared with those obtained from control cells ($P_{Permanova\ (Monte-Carlo)} < 0.05$, Table S1). Exceptions were observed in cells exposed to an intermediate concentration of propranolol (150 µg L^{-1}) and the lowest concentration of dissolved Cu (1 µg L^{-1}) ($P_{Permanova\ (Monte-Carlo)} > 0.05$, Table S1).

Additionally, the dose–response relationships were also analysed for each fatty acid individually under the exposure to the aforementioned treatments (Fig. 2). Fatty acids biosynthesis is a complex process involving several steps. For instance LC-PUFA formation requires insertion of double bonds and elongation of a pre-existing fatty acid (Feijão et al., 2020c). Therefore, increases or decreases on the relative amounts of certain fatty acids are normally followed by a reduction or enhancement of another fatty acid. Several significant correlations emerged between the relative concentrations of multiple fatty acids in each xenobiotic trial. Increasing doses of exogenous bezafibrate lead to a simultaneous significant decrease in the relative concentration of C16:0 ($\rho = -0.38$, $p = 0.02$), C16:4n-1 ($\rho = -0.22$, $p = 0.03$), C18:4n-3 ($\rho = -0.25$, $p = 0.02$) and C20:5n-3 ($\rho = -0.28$, $p = 0.03$), as well as a significant rise in C20:4n-6 ($\rho = 0.32$, $p = 0.01$), in parallel to the bezafibrate applied dose (Fig. 2A). Regarding the cells exposed to fluoxetine, the effects in the individual fatty acid trends were more pronounced. The

Table 2
Specific growth rate and growth inhibition (average values, N = 3 per treatment) observed in the diatom cultures exposed to different xenobiotics and exogenous concentrations tested. Negative growth inhibition values indicate a growth promotion.

Xenobiotic	Concentration	Specific growth rate	Growth inhibition (%)	Reference
Bezafibrate	0 µg L^{-1}	0.70	0%	(Duarte et al., 2019b)
	3 µg L^{-1}	0.85	−39%	
	6 µg L^{-1}	0.68	−27%	
	30 µg L^{-1}	0.78	−98%	
	60 µg L^{-1}	0.82	−127%	
	300 µg L^{-1}	0.72	−50%	
Fluoxetine	0 µg L^{-1}	0.85	0%	(Feijão et al., 2020a)
	0.3 µg L^{-1}	0.86	7%	
	0.6 µg L^{-1}	1.05	10%	
	20 µg L^{-1}	1.19	25%	
	40 µg L^{-1}	0.76	39%	
	80 µg L^{-1}	1.20	83%	
Propranolol	0 µg L^{-1}	0.92	0%	(Duarte et al., 2020b)
	0.3 µg L^{-1}	0.93	19%	
	8 µg L^{-1}	0.94	−2%	
	80 µg L^{-1}	0.82	31%	
	150 µg L^{-1}	1.07	69%	
	300 µg L^{-1}	0.89	56%	
Ibuprofen	0 µg L^{-1}	0.84	0%	
	0.8 µg L^{-1}	0.86	17%	
	3 µg L^{-1}	0.88	20%	(Silva et al., 2020a)
	40 µg L^{-1}	0.87	18%	
	100 µg L^{-1}	1.03	38%	
	300 µg L^{-1}	1.08	40%	
Glyphosate	0 µg L^{-1}	0.84	0%	(de Carvalho et al., 2020)
	10 µg L^{-1}	0.86	−1%	
	50 µg L^{-1}	0.87	21%	
	100 µg L^{-1}	0.92	28%	
	250 µg L^{-1}	0.45	76%	
	500 µg L^{-1}	0.21	89%	
SDS	0 mg L^{-1}	0.84	0%	(Duarte et al., in prep)
	0.1 mg L^{-1}	0.80	15%	
	1 mg L^{-1}	0.78	21%	
	3 mg L^{-1}	0.77	25%	
	10 mg L^{-1}	0.70	44%	
Triclosan	0 µg L^{-1}	0.77	0%	(Duarte et al., in prep)
	0.1 µg L^{-1}	0.63	9%	
	1 µg L^{-1}	0.84	15%	
	10 µg L^{-1}	1.03	11%	
	50 µg L^{-1}	1.33	5%	
	100 µg L^{-1}	1.12	14%	
Dissolved Cu	0 µg L^{-1}	0.71	0%	(Franzitta et al., 2020)
	1 µg L^{-1}	0.64	12%	
	5 µg L^{-1}	0.55	24%	
	10 µg L^{-1}	0.49	34%	
Cu NP	0 µg L^{-1}	0.71	0%	(Franzitta et al., 2020)
	1 µg L^{-1}	0.54	21%	
	5 µg L^{-1}	0.45	33%	
	10 µg L^{-1}	0.28	58%	

increasing fluoxetine dose led to a concomitant decrease in C16:0 ($\rho = -0.74$, $p = 0.0001$), C16:1n-7 ($\rho = -0.59$, $p = 0.0002$), C18:3n-6 ($\rho = -0.47$, $p = 0.0002$) and C18:4n-3 ($\rho = -0.68$, $p = 0.0001$) (Fig. 2B). On the other hand, this pharmaceutical compound led to proportional significant increase in C16:2n-7 ($\rho = 0.86$, $p < 0.00001$), C16:3n-4 ($\rho = 0.94$, $p < 0.00001$) and C20:5n-3 ($\rho = 0.69$, $p < 0.0001$) fatty acids (Fig. 2B). The tests using propranolol as an exogenous stimulus, also led to significant dose–response trends, namely a significant reduction of C14:0 ($\rho = -0.45$, $p = 0.008$), C16:0 ($\rho = -0.55$, $p = 0.0002$), C18:4n-3 ($\rho = -0.50$, $p = 0.04$) and C20:4n-6 ($\rho = -0.40$, $p = 0.02$) (Fig. 2C). The fatty acids C16:2n-7 ($\rho = 0.45$, $p = 0.001$), C16:3n-4 ($\rho = 0.50$, p = 0.0005), C18:3n-6 ($\rho = 0.20$, $p = 0.01$) and C20:5n-3 ($\rho = 0.58$, $p = 0.0001$) showed a positive trend with the exogenous propranolol concentration applied (Fig. 2C). Increasing Ibuprofen concentrations lead to a proportional and significant decrease in the relative concentrations of C14:0 ($\rho = -0.49$, $p = 0.01$) and C16:0 ($\rho = -0.43$, $p = 0.03$) fatty acids and
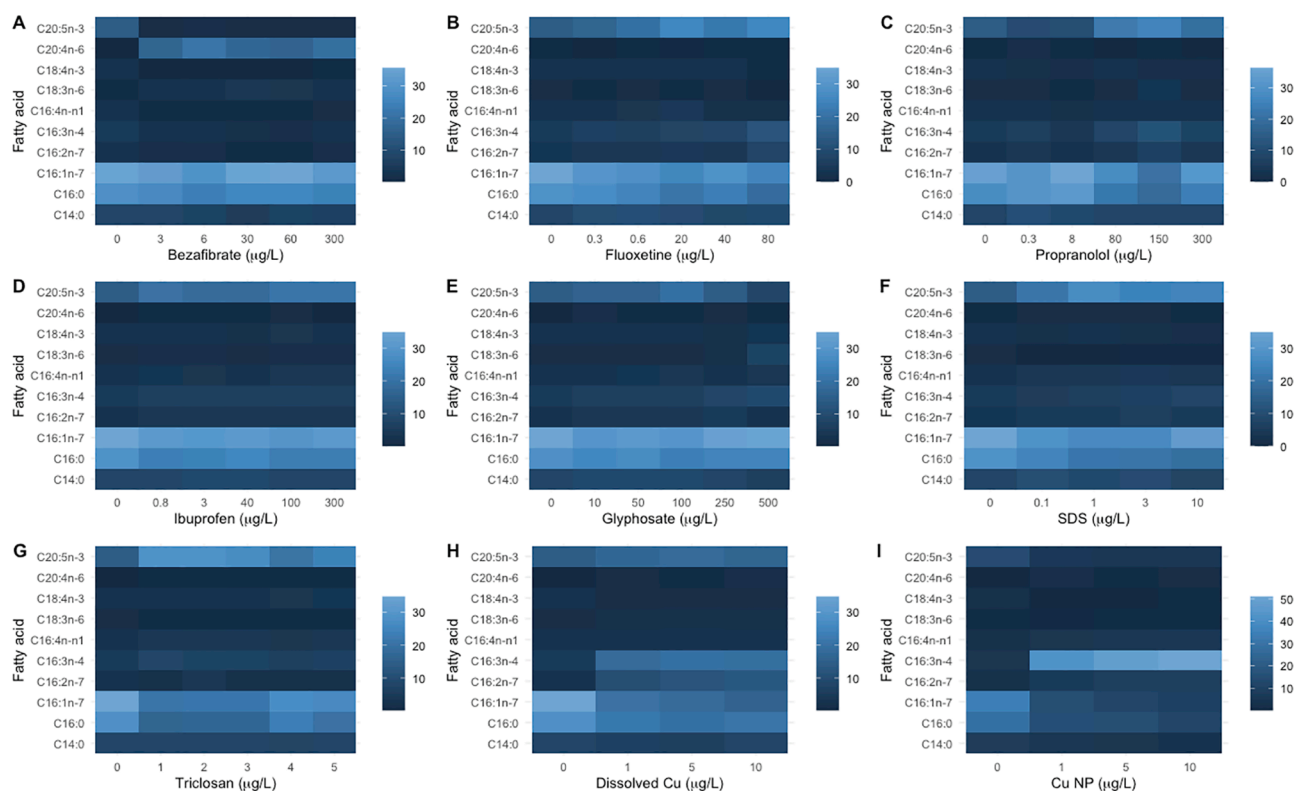
Fig. 1. Relative fatty acid concentration heatmaps of the diatom cells exposed to different xenobiotics (bezafibrate, A; fluoxetine, B; propranolol, C; ibuprofen, D; glyphosate, E; SDS, F; triclosan, G; dissolved Cu, H; Cu nanoparticle (NP), I) and respective concentrations (average, n = 3 per treatment).

increase in the relative concentrations of C16:4n-1 ($\rho = 0.49$, $p = 0.002$), C18:3n-6 ($\rho = 0.49$, $p = 0.001$) and C20:5n-3 ($\rho = 0.48$, $p = 0.02$) fatty acids (Fig. 2D). The pesticide glyphosate induced a significant and proportional depletion in the concentration of C14:0 ($\rho = -0.83$, $p < 0.0001$) and C20:5n-3 ($\rho = -0.64$, $p = 0.002$) fatty acids, while at the same time a positive correlation was observed between the C16:3n-4 ($\rho = 0.68$, $p = 0.003$) and C18:3n-6 ($\rho = 0.56$, $p = 0.01$) fatty acids concentrations and this biocide exogenous concentrations (Fig. 2E). Contrarily to what might be expectable, exposure to the two antimicrobial tested (SDS, Fig. 2F and Triclosan induced different dose–effect relationships.). More specifically, SDS exposure induced a decrease in C16:0 ($\rho = -0.69$, $p = 0.0007$) and C18:4n-3 ($\rho = -0.43$, $p = 0.009$) fatty acids, while under triclosan exposure this negative effect was more pronounced in the C16:2n-7 ($\rho = -0.36$, $p = 0.001$), C16:3n-4 ($\rho = -0.44$, $p < 0.0001$), C18:3n-6 ($\rho = -0.30$, $p = 0.03$) and C20:4n-6 ($\rho = -0.30$, $p = 0.02$) fatty acids. On the other hand, a significant enhancement of the relative concentration of C16:3n-4 ($\rho = 0.84$, $p < 0.0001$) and C20:5n-3 ($\rho = 0.36$, $p = 0.02$) under SDS exposure was found, whereas a significant increase with the applied dose of C18:4n-3 ($\rho = 0.55$, $p < 0.0001$) fatty acid was found in the diatom cells exposed to triclosan. The two copper forms applied also showed very different dose–effect trends (Dissolved Cu, Fig. 2H and Cu nanoparticles, Fig. 2I). Dissolved copper exposure induced mild alterations, with only significant dose–effect depletion in the C16:1n-7 ($\rho = -0.60$, $p < 0.0001$), C18:3n-6 ($\rho = -0.22$, $p = 0.03$) and C18:4n-3 ($\rho = -0.48$, $p < 0.0001$) fatty acids being found. A significant and positive correlation between the dissolved Cu concentrations applied and C16:3n-4 ($\rho = 0.38$, $p = 0.003$) and C16:4n-1 ($\rho = 0.32$, $p = 0.01$) fatty acids relative concentration could also be observed. Regarding Cu nanoparticle exposure, the cells exhibited a strong pattern of influence of this metal form in all fatty acid concentrations, showing an inverse significant correlation with the Cu applied dose ($\rho_{C14:0} = -0.67$, $\rho_{C16:0} = -0.70$, $\rho_{C16:1n-7} = -0.75$, $\rho_{C18:3n-6} = -0.62$, $\rho_{C18:4n-3} = -0.50$, $\rho_{C20:4n-6} = -0.45$, $\rho_{C20:5n-3} = -0.60$, $p < 0.001$ in all cases), apart from

C16:2n-7 ($\rho = 0.50$, $p < 0.0001$), C16:3n-4 ($\rho = 0.70$, $p < 0.0001$) and C16:4n-1 ($\rho = 0.76$, $p < 0.0001$) that showed the inverse trend.

3.3. Fatty acids profiles under different xenobiotic exposures

Considering the diverse individual relationships observed between fatty acid concentrations and the exogenous concentration of each xenobiotic applied becomes important to address the fatty acids as a whole profile to better classify the toxicity degrees of the samples. For this purpose, a multivariate approach was conducted using Canonical Analysis of Principal (CAP) components for each of the xenobiotics applied, using the fatty acid relative concentration as canonical vectors (Figs. 3 and 4). When observing the canonical distribution of the fatty acid profiles of the samples regarding the type of xenobiotic applied, some clear separations are evident, highlighting the different impacts of each of the exposure treatments (Fig. 3). The samples exposed to bezafibrate appeared separated from the remaining groups, mostly due to a higher relative concentration of the C16:1n-7 fatty acid and reduced C16:2n-7 and C16:3n-4. A second group formed by all the samples exposed to non-metallic xenobiotics (pharmaceuticals, detergents, and biocides) also emerged in the CAP diagram, associated with high C20:5n-3 and low C20:4n-6 relative concentrations. Interestingly, the group formed by the samples exposed to the two tested Cu treatments (dissolved Cu and Cu nanoparticles) was separated from the rest of the tested treatments and also from each other. Cultures exposed to Cu NP were grouped according to their higher relative content in C16:3n-4 and C16:2n-7 fatty acids, while the cluster formed by the samples exposed to dissolved Cu were mostly associated with higher relative concentrations of C16:4n-1 and low C20:4n-6 contents. Furthermore, the fatty acid profiles of the samples showed a canonical classification efficiency of 73.3 % regarding the type of treatment to which the cells were exposed, indicating a xenobiotic exposure specific fatty acid profile.

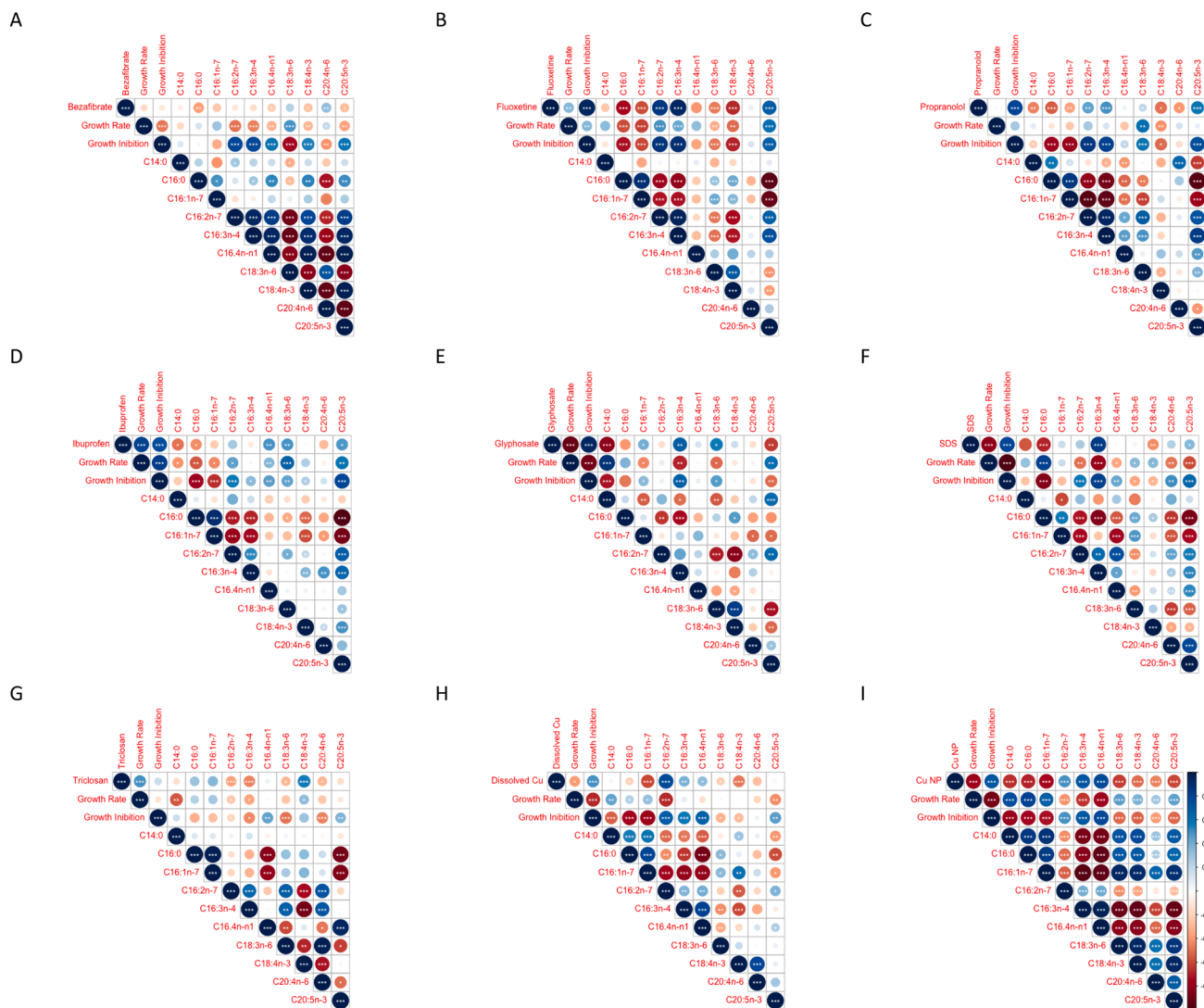The exposure of the diatom cultures to bezafibrate (Fig. 4A) had very

Fig. 2. Fatty acid relative concentrations, growth rate and inhibition Spearman correlograms relative to the diatom cells exposed to different xenobiotics (bezafibrate, A; fluoxetine, B; propranolol, C; ibuprofen, D; glyphosate, E; SDS, F; triclosan, G; dissolved Cu, H; Cu nanoparticle (NP), I) and respective concentrations (asterisks denote significant correlations at * p < 0.05, ** p < 0.01 and *** p < 0.001).

similar impacts among t4ested concentrations, allowing only the differentiation of the control samples versus the bezafibrate exposed samples (canonical classification efficiency = 50 %). This differentiation was mainly due to the higher content of C16:3n-4, C16:4n-1 and C18:4n-3 fatty acids in the control samples when compared to those exposed to this lipid regulator. On the other hand, the application of the antidepressant fluoxetine led to distinct diatom fatty acid profiles along the exposure gradient (Fig. 4B). This resulted in a canonical plot with a high degree of classification efficiency regarding the applied exogenous concentration (83.3 %). The most evident separation is observed in the groups formed by the samples belonging to the control group versus the cells exposed to the highest drug concentration (80 μg L^{-1}). Under high exposure to fluoxetine, higher percentages of C16:2n-7 and C16:3n-4 were detected in the cells. With the intermediate concentrations tested, some degree of overlapping could be observed particularly within the samples exposed to 0.3 μg L^{-1} and 0.6 μg L^{-1} and the samples exposed to 20 μg L^{-1} and 40 μg L^{-1}, indicating mild effects in these two sample treatment groups. Under propranolol exposure, the diatom fatty acid profiles acquired more distinctive characteristics between exposure doses (Fig. 4C). Apart from the cells exposed to the medium and high propranolol concentrations tested (80 and 300 μg L^{-1}), all the exposed groups appear clearly individualized, indicating a high degree of

specificity of the fatty acid profiles related to the applied propranolol dose (canonical classification efficiency = 88.9 %). This clear separation is mostly driven by changes in the LC-PUFA C20:4n-6 and C20:5n-3, with these two canonical vectors showing a higher influence in separating the control samples and those exposed to low propranolol exogenous concentrations (0.3 and 8 μg L^{-1}) from the samples exposed to the highest tested doses (80, 150 and 300 μg L^{-1}). Ibuprofen-induced fatty acid profiles (Fig. 4D) also clearly separated samples exposed to different treatments, though presenting some overlap in the samples exposed to mild (40 and 100 μg L^{-1}) concentrations (canonical classification efficiency = 61.1 %). Samples exposed to low (0.8 and 3 μg L^{-1}) ibuprofen concentrations appear associated with higher C14:0 relative concentrations, which was reduced with the increasing exogenous ibuprofen concentration tested. The exposure of the test diatoms to mild glyphosate concentrations (10, 50 and 100 μg L^{-1}) resulted in similar fatty acid profiles (Fig. 4E), mostly influenced by higher relative concentrations of C16:0 and C16:4n-1 fatty acids in the cells exposed to these concentrations of glyphosate. This overlap resulted in a decrease in the overall canonical classification (canonical classification efficiency = 55.6 %). The samples exposed to 250 μg glyphosate L^{-1} were clearly grouped mostly due to a reduction in the relative C20:4n-6 concentration, while the samples exposed to 500 μg glyphosate L^{-1} were grouped
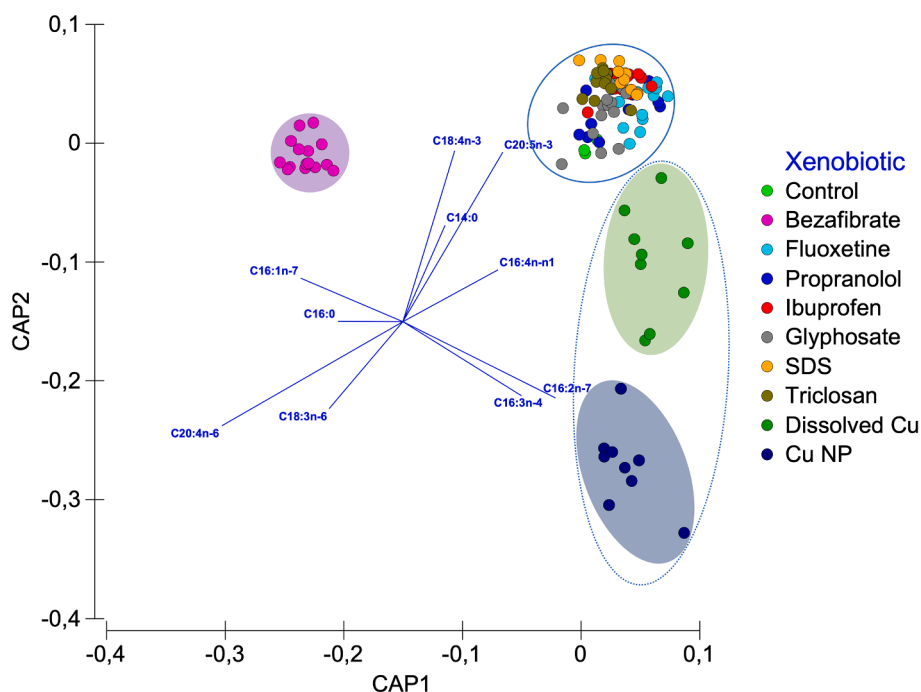
Fig. 3. Canonical Analysis of Principal (CAP) components based in the diatom cells fatty acid profiles exposed to the different tested xenobiotics.

due to their lower concentration in C14:0, C18:4n-3 and C20:5n-3. Regarding the samples exposed to the antimicrobial detergent SDS, the fatty acid profiles of the samples also revealed a high degree of specificity regarding the treatment applied, with an overall canonical classification efficiency of 73.3 % (Fig. 4F). The samples exposed to the highest SDS concentration were mostly differentiated due to high concentration in C16:1n-7 and low relative abundances of C16:0, C14:0 and C18:4n-3 fatty acids found in the cells. The latter corresponds to the biochemical traits that group cells exposed to 0.1 and 3 mg L^{-1} SDS. The other antimicrobial detergent tested, triclosan, showed a canonical plot (Fig. 4G) very similar to that observed under bezafibrate exposure, with only an evident separation between the control and exposed samples, leading to a very low degree of classification efficiency (27.8 %). Finally, under Cu exposure, there is a clear differentiation between the cells exposed to the two different forms of Cu tested and also between the Cu treatments and the control group (Fig. 4H). More specifically, the samples exposed to dissolved Cu treatments are grouped by their higher C16:2n-7 concentration, while the samples exposed to Cu NP have this fatty acid concentration reduced concomitantly with increased levels of C16:3n-4 and C16:4n-1. Regarding the individual exposure to each of the Cu forms tested, the fatty acid profiles of the samples revealed 58.3 % and 66.7 % classification efficiencies, for the cultures exposed to dissolved Cu and Cu NP (data not shown), respectively.

3.4. LipidTOX integrated biomarker response index

Applying the IBR calculation pipeline, it was possible to construct specific indexes for each of the xenobiotic exposure trials (Fig. 5). Overall, an increasing exogenous dose of any of the tested xenobiotics led to an increased index value. This was particularly evident in the samples exposed to fluoxetine (Fig. 5B), propranolol (Fig. 5C), ibuprofen (Fig. 5D), SDS (Fig. 5F), triclosan (Fig. 5G) and Cu NP (Fig. 5I), where the highest applied dose resulted in significantly high values not only when compared with the control treatment but also with the lowest doses applied. In fact, the rising index value with increasing exposure doses pointed out to possible direct dose–effect correlation with the index. To confirm this assumption and evaluate the efficiency of the index as a sensible descriptor of the ecotoxicological effects of exposure,

the index value correlation between the exogenous dose applied and the cells growth rate and inhibition was evaluated (Fig. 6). For this purpose, a normalized index (n-LipidTOX) was also computed using the index deviation to the control samples, to evaluate if a normalization factor could improve the index efficiency in relation to the exogenous dose applied and to the cells growth rate and inhibition. Regarding the indexes behaviour, when compared to the exogenous dose applied, a direct correlation was observed with all the compounds tested, which was more significant in the samples exposed to fluoxetine ($\rho = 0.90$, $p = 0.02$ for both index versions) (Fig. 6B), glyphosate ($\rho = 0.88$, $p = 0.002$ for both index versions) (Fig. 6E), SDS ($\rho = 0.80$, $p = 0.004$ for both index versions) (Fig. 6F) and Cu NP ($\rho = 0.86$, $p = 0.002$ for both index versions) (Fig. 6I). Comparison of the trends observed between the index values obtained (either in raw or normalized version) with the growth rate, showed an inverse significant correlation in the samples exposed to glyphosate ($\rho = -0.92$, $p < 0.0001$ for both index versions) (Fig. 6E), SDS ($\rho = -0.83$, $p = 0.002$ for both index versions) (Fig. 6F) and Cu NP ($\rho = -0.78$, $p < 0.004$ for both index versions) (Fig. 6I). When comparing the index values with the growth inhibition data, it was possible to observe a strong and significant relationship in these same treatments ($\rho_{fluoxetine} = 0.89$, $p < 0.03$; $\rho_{glyphosate} = 0.74$, $p = 0.01$; $\rho_{SDS} = 0.87$, $p < 0.0001$; $\rho_{Cu NP} = -0.75$, $p = 0.001$). Although lacking statistical significance for the remaining studied cases, it is worth noticing the high values of the correlation coefficient between the index values obtained and the exogenous doses applied and the cultures growth features. Regarding the index normalization using the control, it did not change the relationship between the index value computed and the cultures growth and exposure features.

4. Discussion

Contaminants, when occurring above certain thresholds, can induce physiological constraints to organisms (Anjum et al., 2016; Cruz de Carvalho et al., 2020b; Duarte et al., 2013; Duarte et al., 2020a), leading to the triggering of feedback mechanisms that can be used as biomarkers of xenobiotic exposure, such as changes in antioxidant response systems (Duarte et al., 2013; Pires et al., 2021), primary photochemistry (Cruz de Carvalho et al., 2020a; Duarte et al., 2021b) or fatty acid profiles (Duarte
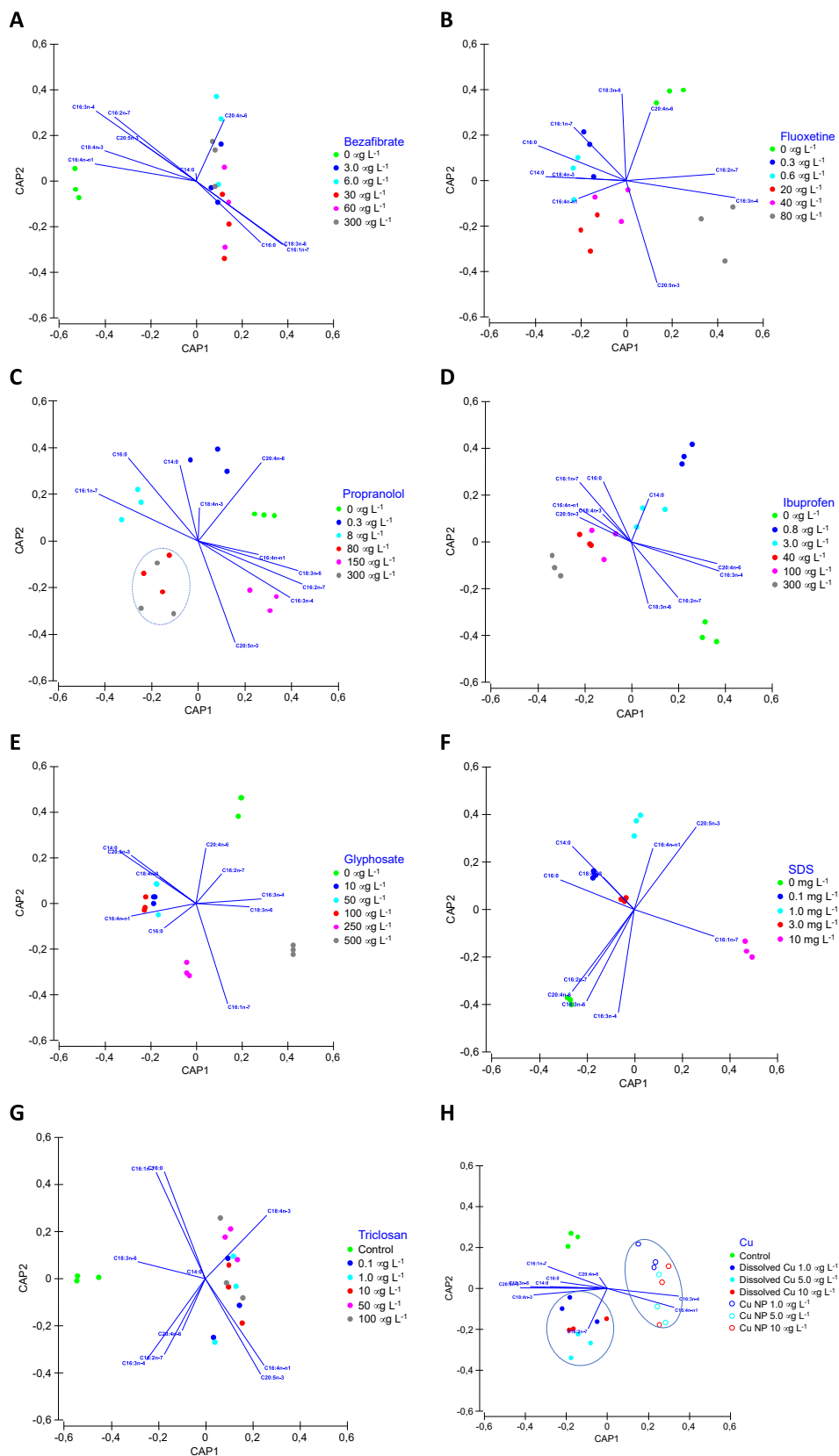
Fig. 4. Canonical Analysis of Principal (CAP) components based on the diatom cells fatty acid profiles exposed to the different tested xenobiotics and concentrations (bezafibrate, A; fluoxetine, B; propranolol, C; ibuprofen, D; glyphosate, E; SDS, F; triclosan, G; dissolved Cu and Cu nanoparticle (NP), H).
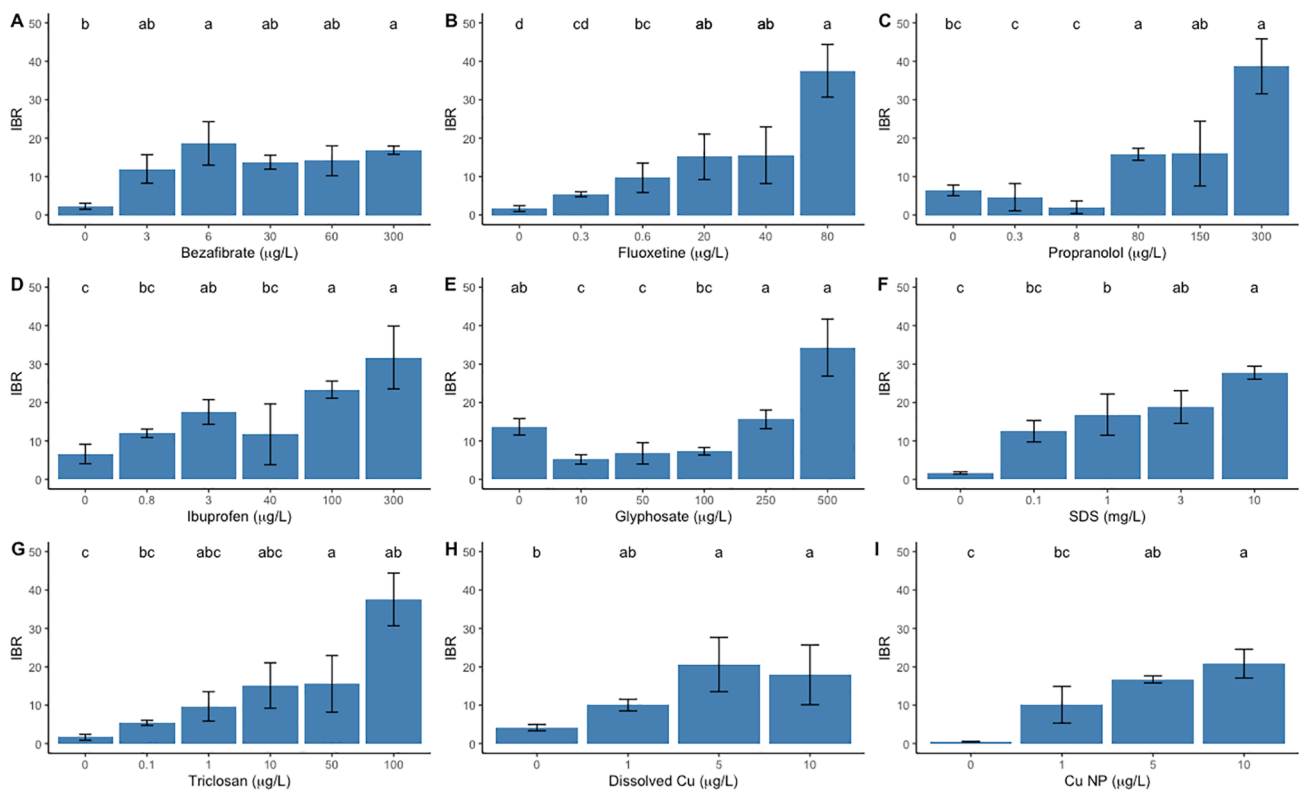
Fig. 5. Fatty acid-based integrated biomarker response (IBR) index values for the diatom cells exposed to the different xenobiotics and tested concentrations (bezafibrate, A; fluoxetine, B; propranolol, C; ibuprofen, D; glyphosate, E; SDS, F; triclosan, G; dissolved Cu, H; Cu nanoparticle (NP), I) and respective concentrations (average ± standard deviation, N = 3 per treatment, different letters denote significant differences at p < 0.05 between exposure treatments).

et al., 2018a; Duarte et al., 2021a). Although xenobiotic exposure affects the entire trophic web, triggers multiple and sometimes species-specific alterations, depending on the organisms affected (Brausch et al., 2012; Lopes et al., 2020; Pires et al., 2021; Roma et al., 2020), the impacts of xenobiotics acquire an even more critical aspect at the basis of the trophic web, imposing direct and indirect serious ecosystem shifts. These effects will impact directly the marine communities by affecting the phytoplanktonic compartment functioning and abundance, or due to the inevitable reduction of the energy fluxes (in the form of carbohydrates, fatty acids and other essential nutrients to the upper trophic levels) and oxygen provided by this group of organisms (Duarte et al., 2020; Cabrita et al., 2016; Feijão et al., 2020a). As above mentioned, diatoms are also a source of essential fatty acids (Jónasdóttir, 2019). Additionally, fatty acids have also proved to be a suitable source of biomarkers towards environmental stresses (Duarte et al., 2018c; Duarte et al., 2019a; Duarte et al., 2020d; Feijão et al., 2020c) but also of contaminant exposure, especially in marine diatoms (Cruz de Carvalho et al., 2020c; Duarte et al., 2020b; Feijão et al., 2020a; Franzitta et al., 2020; Silva et al., 2020a). This reinforces the potential of integrating these very important molecules from these key organisms into an unifying index, that can be further applied in risk assessment and ecotoxicological studies.

In the present work, it is well patent the diverse impacts of the different xenobiotics and the respective doses applied in the model marine diatom *P. tricornutum*. Aside from the physiological meaning of the changes induced by these contaminants, the resulting fatty acids arise as a pool of potentially useful biomarkers that cannot be disregarded. In terms of the impacts at the fatty acid individual level, it is possible to observe that this can go from highly transversal effects, such as the reduction of C14:0 and C16:0 fatty acids relative amounts with increasing xenobiotic concentration, as observed for example under propranolol and fluoxetine exposure (Duarte et al., 2020b; Feijão et al.,

2020a), to an enhancement of the proportions of C16:2n-7 and C16:3n-4 fatty acids (de Carvalho et al., 2020; Feijão et al., 2020a; Franzitta et al., 2020) or complete disruption of the fatty acid profile as observed in the diatoms exposed to copper nanoparticles (Franzitta et al., 2020). These diverse alterations in fatty acid concentrations, appear to be highly dependent not only on the xenobiotic applied but also on the tested concentration. Moreover, these alterations appear intrinsically connected due to the interconversion of several fatty acids into each other, highlighting the need to address these profiles as a whole, instead of the classical individual fatty acid analysis approach. An alteration in a certain fatty acid concentration, either directly by, for example, oxidative stress imposed by the stressor or indirectly through their use by enzymes that catalyse its conversion in another fatty acid, impacts not only the fatty acid itself but also its metabolic precursors and products and thus affect the cell's whole fatty acid profile (Feijão et al., 2020c; Laureano et al., 2018; Matos et al., 2007).

Looking into the fatty acid profiles of diatoms through a multivariate approach, revealed that this set of biochemical traits efficiently disclosed the type of xenobiotic applied to the diatoms, clearly separating three major canonical groups. The first was composed by the cells exposed to bezafibrate, the only pharmaceutical compound tested that acts as a lipid regulator (Duarte et al., 2019b), suggesting a potentially specific and direct impact of this compound on the fatty acid profile of the diatoms, which was particularly distinct from the remaining tested substances. A second group was found to be composed of the samples exposed to Cu, the only trace element examined among the array of tested xenobiotics, with two individualized clusters corresponding to the cells subjected to the two tested forms of Cu: dissolved and nanoparticles. This cluster separation is likely to be related to the higher toxic effect of metal oxide nanoparticles on cells in comparison with their dissolved (ionic) counterparts at similar concentrations and also to different biochemical changes induced by the two metal forms (Franzitta
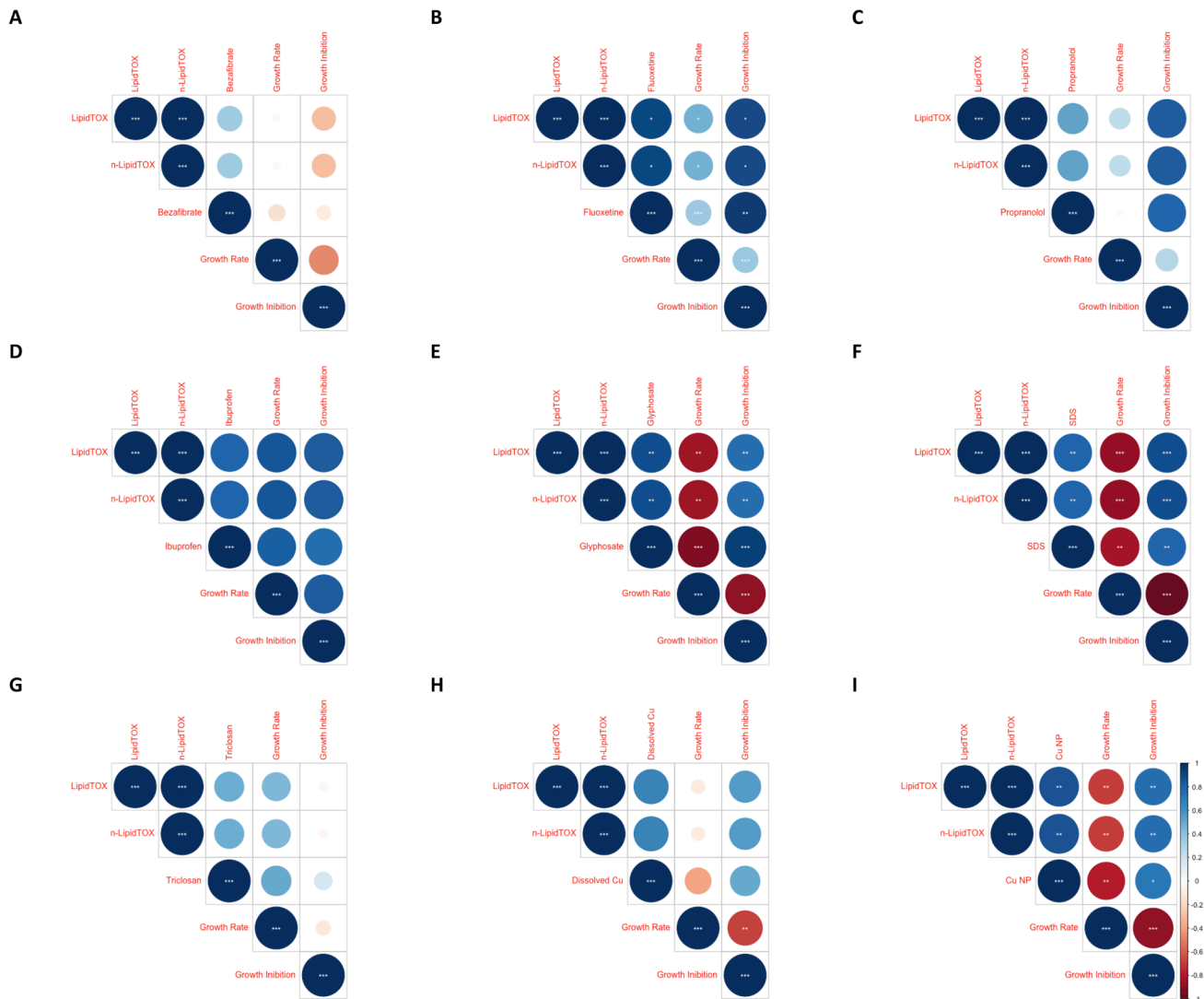
Fig. 6. LipidTOX index, xenobiotic exogenous concentration, growth rate and inhibition Spearman correlograms relative to the diatom cells exposed to the different xenobiotics (bezafibrate, A; fluoxetine, B; propranolol, C; ibuprofen, D; glyphosate, E; SDS, F; triclosan, G; dissolved Cu, H; Cu nanoparticle (NP), I) and respective concentrations (asterisks denote significant correlations at * $p < 0.05$, ** $p < 0.01$ and *** $p < 0.001$).

et al., 2020). This highlights the sensitivity of the diatom fatty acids, facilitating the differentiation between xenobiotics and even forms of the same xenobiotic. Trace elements are known to alter cells when occurring in toxic concentrations, by inducing oxidative stress (Anjum et al., 2016; Kumar et al., 2010). Although organic contaminants such as detergents, biocides and pharmaceutical compounds, can also cause oxidative stress, they are also metabolized by the cells and generate indirect metabolic changes (de Carvalho et al., 2020; Duarte et al., 2019b; Duarte et al., 2020).

Analysing the fatty acid profiles along the xenobiotic concentration ranges tested, once again revealed a high degree of efficiency in discriminating sample groups exposed to different xenobiotic concentrations. Nevertheless, some degree of overlap could be found in very low or extremely high xenobiotic concentrations in the cultures exposed to some types of xenobiotics. Effects of xenobiotics' concentrations occurring below and above certain thresholds values were not detected, either because the exogenous concentration applied did not surpass the cells tolerance limit or the maximum tolerance threshold was already surpassed and thus no additional effects are observed, as it was found in previous studies and as highlighted by the growth rate and inhibition (de Carvalho et al., 2020; Duarte et al., 2020c; Silva et al., 2020a).

Similarly to what has been previously proposed with other

biomarker sets such as photochemistry (Cruz de Carvalho et al., 2020a) and classical enzymatic biomarkers (Pires et al., 2021), gathering these biochemical traits into unifying numerical indexes has proven to be an efficient approach in translating the organisms' stress condition into a single numerical value. This index approach using fatty acid profiles has already been developed for macroalgae (Duarte et al., 2021a) and higher plants (Duarte et al., 2018a), and was here successfully applied for marine diatoms. Having this in mind, a classical index elaboration procedure [integrated biomarker response index (Beliaeff and Burgeot, 2002b) was employed using the fatty acid concentrations in the diatoms exposed to the different test conditions – the LipidTOX index. Two approaches were undertaken: 1) classic IBR calculation for the control and exposed samples, and 2) a normalized version of the index integrating the deviation of the exposed samples towards the respective control condition. This last version was undertaken to integrate potential and subtle differences from the control cultures performed simultaneously with each xenobiotic exposure. Nevertheless, it was found that these two approaches produced similar tendencies when compared to the measured growth traits. According to the OECD guidelines (OECD, 2011), these growth features are considered to be good indicators of the ecotoxicological effects of a certain xenobiotic in microalgae. Our results show that, in most cases, the LipidTOX index (either in its classical or

normalized version) is highly efficient in translating the growth impairments imposed by each of the xenobiotics tested including at different test concentrations. Additionally, it was also found that the generated indexes also presented very good correlations with the known exogenous dose applied. The results from this study highlight the efficiency of the LipidTOX index in translating the ecotoxicological effects imposed by the different xenobiotics into a single numerical value, that can be easily addressed by a non-expert audience.

5. Conclusions

Diatom fatty acids are suitable to be included in unifying indexes, such as the one proposed in the present study. The LipidTOX index was proven to be an efficient tool for ecotoxicological assays using marine model diatoms and evidenced a high degree of reliability for classifying the exposure of the cells to emerging contaminants. Additionally, the index development methodology here proposed as well as the LipidTOX index itself, can be easily applied to other autotrophic organisms, subjected to different stress conditions, once calibrated, and validated against known biochemical or morphological descriptors of stress. Thus, complex fatty acid profiles are integrated into a unifying numerical index that can be easily communicated to non-expert audiences such as stakeholders, policymakers, and environmental managers for future toxicological evaluations of the impacts of classical and emerging xenobiotics in marine primary producers.

CRediT authorship contribution statement

Bernardo Duarte: Investigation, Data curation, Formal analysis, Funding acquisition, Project administration, Writing – original draft. **Eduardo Feijão:** Investigation, Writing – review & editing. **Marco Franzitta:** Investigation, Writing – review & editing. **Irina A. Duarte:** Investigation, Writing – review & editing. **Ricardo Cruz de Carvalho:** Investigation, Writing – review & editing. **Maria Teresa Cabrita:** Writing – review & editing. **João Carlos Marques:** Writing – review & editing. **Isabel Caçador:** Writing – review & editing. **Vanessa Fonseca:** . **Ana Rita Matos:** Supervision, Writing – review & editing.

Declaration of Competing Interest

The authors declare that they have no known competing financial interests or personal relationships that could have appeared to influence the work reported in this paper.

Acknowledgements

Appendix A. Supplementary data

Supplementary data to this article can be found online at https://doi.org/10.1016/j.ecolind.2022.108885.

References

Alygizakis, N.A., Gago-Ferrero, P., Borova, V.L., Pavlidou, A., Hatzianestis, I., Thomaidis, N.S., 2016. Occurrence and spatial distribution of 158 pharmaceuticals, drugs of abuse and related metabolites in offshore seawater. Sci. Total Environ. 541, 1097–1105. https://doi.org/10.1016/j.scitotenv.2015.09.145.

Aminot, Y., Fuster, L., Pardon, P., Le Menach, K., Budzinski, H., 2018. Suspended solids moderate the degradation and sorption of waste water-derived pharmaceuticals in estuarine waters. Sci. Total Environ. 612, 39–48. https://doi.org/10.1016/j.scitotenv.2017.08.162.

Anjum, N.A., Duarte, B., Caçador, I., Sleimi, N., Duarte, A.C., Pereira, E., 2016. Biophysical and biochemical markers of metal/metalloid-impacts in salt marsh halophytes and their implications. Front. Environ. Sci. 4, 1–13. https://doi.org/10.3389/fenvs.2016.00024.

aus der Beek, T., Weber, F.A., Bergmann, A., Hickmann, S., Ebert, I., Hein, A., Küster, A., 2016. Pharmaceuticals in the environment-Global occurrences and perspectives. Environ. Toxicol. Chem. 35, 823–835. https://doi.org/10.1002/etc.3339.

Beliaeff, B., Burgeot, T., 2002a. In: Integrated biomarker response: A useful tool for ecological risk assessment, in: Environmental Toxicology and Chemistry. SETAC Press, pp. 1316–1322. https://doi.org/10.1002/etc.5620210629.

Beliaeff, B., Burgeot, T., 2002. Integrated biomarker response: a useful tool for ecological risk assessment. Environ. Toxicol. Chem./SETAC 21, 1316–1322. https://doi.org/10.1002/etc.5620210629.

Bowler, C., Allen, A.E., Badger, J.H., Grimwood, J., Jabbari, K., Kuo, A., Maheswari, U., Martens, C., Maumus, F., Otillar, R.P., Rayko, E., Salamov, A., Vandepoele, K., Beszteri, B., Gruber, A., Heijde, M., Katinka, M., Mock, T., Valentin, K., Verret, F., Berges, J.A., Brownlee, C., Cadoret, J.P., Chiovitti, A., Choi, C.J., Coesel, S., De Martino, A., Detter, J.C., Durkin, C., Falciatore, A., Fournet, J., Haruta, M., Huysman, M.J.J., Jenkins, B.D., Jiroutova, K., Jorgensen, R.E., Joubert, Y., Kaplan, A., Kröger, N., Kroth, P.G., La Roche, J., Lindquist, E., Lommer, M., Martin-Jézéquel, V., Lopez, P.J., Lucas, S., Mangogna, M., McGinnis, K., Medlin, L.K., Montsant, A., Secq, M.P.O.L., Napoli, C., Obornik, M., Parker, M.S., Petit, J.L., Porcel, B.M., Poulsen, N., Robison, M., Rychlewski, L., Rynearson, T.A., Schmutz, J., Shapiro, H., Siaut, M., Stanley, M., Sussman, M.R., Taylor, A.R., Vardi, A., Von Dassow, P., Vyverman, W., Willis, A., Wyrwicz, L.S., Rokhsar, D.S., Weissenbach, J., Armbrust, E.V., Green, B.R., Van De Peer, Y., Grigoriev, I.V., 2008. The Phaeodactylum genome reveals the evolutionary history of diatom genomes. Nature 456, 239–244. https://doi.org/10.1038/nature07410.

Brausch, J.M., Connors, K.A., Brooks, B.W., Rand, G.M., 2012. Human Pharmaceuticals in the Aquatic Environment: A Review of Recent Toxicological Studies and Considerations for Toxicity Testing. In: Whitacre, D.M. (Ed.), Reviews of Environmental Contamination and Toxicology. Springer US, Boston, MA, pp. 1–99. https://doi.org/10.1007/978-1-4614-3137-4_1.

Broeg, K., Lehtonen, K.K., 2006. Indices for the assessment of environmental pollution of the Baltic Sea coasts: Integrated assessment of a multi-biomarker approach. Mar. Pollut. Bull. 53, 508–522. https://doi.org/10.1016/j.marpolbul.2006.02.004.

Cabrita, M.T., Duarte, B., Gameiro, C., Godinho, R.M., Caçador, I., 2018. Photochemical features and trace element substituted chlorophylls as early detection biomarkers of metal exposure in the model diatom Phaeodactylum tricornutum. Ecol. Ind. 95, 1038–1052. https://doi.org/10.1016/j.ecolind.2017.07.057.

Cabrita, M.T., Duarte, B., Gameiro, C., Godinho, R.M., Caçador, I., 2017. Photochemical features and trace element substituted chlorophylls as early detection biomarkers of metal exposure in the model diatom Phaeodactylum tricornutum. Ecol. Ind. 0–1 https://doi.org/10.1016/j.ecolind.2017.07.057.

Cabrita, M.T., Gameiro, C., Utkin, A.B., Duarte, B., Caçador, I., Cartaxana, P., 2016. Photosynthetic pigment laser-induced fluorescence indicators for the detection of changes associated with trace element stress in the diatom model species Phaeodactylum tricornutum. Environ. Monit. Assess. 188, 285. https://doi.org/10.1007/s10661-016-5293-4.

CAS, 2011. CAS REGISTRY Keeps Pace with Rapid Growth of Chemical Research, Registers 60 Millionth Substance. Chemical Abstracts Service, Columbus.

Chen, B., Xue, C., Amoah, P.K., Li, D., Gao, K., Deng, X., 2019. Impacts of four ionic liquids exposure on a marine diatom Phaeodactylum tricornutum at physiological and biochemical levels. Sci. Total Environ. 665, 492–501. https://doi.org/10.1016/j.scitotenv.2019.02.020.

Cid, A., Herrero, C., Torres, E., Abalde, J., 1995. Copper toxicity on the marine microalga Phaeodactylum tricornutum: effects on photosynthesis and related parameters. Aquat. Toxicol. 31, 165–174. https://doi.org/10.1016/0166-445X(94)00071-W.

Claessens, M., Vanhaecke, L., Wille, K., Janssen, C.R., 2013. Emerging contaminants in Belgian marine waters: Single toxicant and mixture risks of pharmaceuticals. Mar. Pollut. Bull. 71, 41–50. https://doi.org/10.1016/j.marpolbul.2013.03.039.

Clarke, K.R., Gorley, R.N., 2006. PRIMER v6: User Manual/Tutorial. PRIMER-E, Plymouth UK 192 p. https://doi.org/10.1111/j.1442-9993.1993.tb00438.x.

Cloern, J.E., 2018. Why large cells dominate estuarine phytoplankton. Limnol. Oceanogr. 63, S392–S409. https://doi.org/10.1002/lno.10749.

Cruz de Carvalho, R., Feijão, E., Kletschkus, E., Marques, J.C., Reis-Santos, P., Fonseca, V.F., Papenbrock, J., Caçador, I., Duarte, B., 2020a. Halophyte bio-optical phenotyping: A multivariate photochemical pressure index (Multi-PPI) to classify salt marsh anthropogenic pressures levels. Ecol. Ind. 119, 106816 https://doi.org/10.1016/j.ecolind.2020.106816.

Cruz de Carvalho, R., Feijão, E., Kletschkus, E., Marques, J.C., Reis-Santos, P., Fonseca, V.F., Papenbrock, J., Caçador, I., Duarte, B., de Carvalho, R., Feijão, E., Kletschkus, E., Marques, J.C., Reis-Santos, P., Fonseca, V.F., Papenbrock, J., Caçador, I., Duarte, B., Cruz de Carvalho, R., Feijão, E., Kletschkus, E., Marques, J.C., Reis-Santos, P., Fonseca, V.F., Papenbrock, J., Caçador, I., Duarte, B., 2020b. Halophyte bio-optical phenotyping: A multivariate photochemical pressure index (Multi-PPI) to classify salt marsh anthropogenic pressures levels. Ecol. Ind. 119, 106816 https://doi.org/10.1016/j.ecolind.2020.106816.

Cruz de Carvalho, R., Feijão, E., Matos, A.R., Cabrita, M.T., Novais, S.C., Lemos, M.F.L., Caçador, I., Marques, J.C., Reis-Santos, P., Fonseca, V.F., Duarte, B., 2020c. Glyphosate-based herbicide toxicophenomics in marine diatoms: Impacts on primary

production and physiological fitness. Appl. Sci. (Switzerland) 10, 1–21. https://doi.org/10.3390/app10217391.

de Carvalho, R.C., Feijão, E., Matos, A.R., Cabrita, M.T., Novais, S.C., Lemos, M.F.L., Caçador, I., Marques, J.C., Reis-Santos, P., Fonseca, V.F., Duarte, B., 2020. Glyphosate-based herbicide toxicophenomics in marine diatoms: Impacts on primary production and physiological fitness. Appl. Sci. (Switzerland) 10, 1–21. https://doi.org/10.3390/app10217391.

De Mendiburu, F., Simon, R., 2015. Agricolae - Ten years of an open source statistical tool for experiments in breeding, agriculture and biology (preprint). PeerJ PrePrints. https://doi.org/10.7287/peerj.preprints.1404v1.

Du, B., Zhang, Z., Liu, W., Ye, Y., Lu, T., Zhou, Z., Li, Y., Fu, Z., Qian, H., 2019. Acute toxicity of the fungicide azoxystrobin on the diatom Phaeodactylum tricornutum. Ecotoxicol. Environ. Saf. 168, 72–79. https://doi.org/10.1016/j.ecoenv.2018.10.074.

Duarte, B., Cabrita, M.T., Vidal, T., Pereira, J.L., Pacheco, M., Pereira, P., Canário, J., Gonçalves, F.J.M., Matos, A.R., Rosa, R., Marques, J.C., Caçador, I., Gameiro, C., 2018a. Phytoplankton community-level bio-optical assessment in a naturally mercury contaminated Antarctic ecosystem (Deception Island). Marine Environ. Res. 140, 412–421. https://doi.org/10.1016/j.marenvres.2018.07.014.

Duarte, B., Carreiras, J., Feijão, E., Reis-Santos, P., Caçador, I., Matos, A.R., Fonseca, V.F., 2021a. Fatty acid profiles of estuarine macroalgae are biomarkers of anthropogenic pressures: Development and application of a multivariate pressure index. Sci. Total Environ. 788, 147817 https://doi.org/10.1016/j.scitotenv.2021.147817.

Duarte, B., Carreiras, J., Pérez-Romero, J.A., Mateos-Naranjo, E., Redondo-Gómez, S., Matos, A.R., Marques, J.C., Caçador, I., 2018. Halophyte fatty acids as biomarkers of anthropogenic-driven contamination in Mediterranean marshes: Sentinel species survey and development of an integrated biomarker response (IBR) index. Ecol. Ind. 87, 86–96. https://doi.org/10.1016/j.ecolind.2017.12.050.

Duarte, B., Durante, L., Marques, J.C., Reis-Santos, P., Fonseca, V.F., Caçador, I., 2021b. Development of a toxicophenomic index for trace element ecotoxicity tests using the halophyte Juncus acutus: Juncus-TOX. Ecol. Ind. 121, 107097 https://doi.org/10.1016/j.ecolind.2020.107097.

Duarte, B., Durante, L., Marques, J.C., Reis-Santos, P., Fonseca, V.F., Caçador, I., 2020b. Development of a toxicophenomic index for trace element ecotoxicity tests using the halophyte Juncus acutus: Juncus-TOX. Ecol. Ind. 121, 107097 https://doi.org/10.1016/j.ecolind.2020.107097.

Duarte, B., Feijão, E., Cruz de Carvalho, R., Franzitta, M., Carlos Marques, J., Caçador, I., Teresa Cabrita, M., Fonseca, V.F., 2021c. Unlocking Kautsky's dark box: Development of an optical toxicity classification tool (OPTOX index) with marine diatoms exposed to emerging contaminants. Ecol. Ind. 131, 108238 https://doi.org/10.1016/j.ecolind.2021.108238.

Duarte, B., Feijão, E., de Carvalho, R.C., Duarte, I.A., Silva, M., Matos, A.R., Cabrita, M.T., Novais, S.C., Lemos, M.F.L., Marques, J.C., Caçador, I., Reis-Santos, P., Fonseca, V.F., 2020c. Effects of propranolol on growth, lipids and energy metabolism and oxidative stress response of phaeodactylum tricornutum. Biology 9, 1–21. https://doi.org/10.3390/biology9120478.

Duarte, B., Gameiro, C., Matos, A.R., Figueiredo, A., Silva, M.S., Cordeiro, C., Caçador, I., Reis-Santos, P., Fonseca, V., Cabrita, M.T., 2021d. First screening of biocides, persistent organic pollutants, pharmaceutical and personal care products in Antarctic phytoplankton from Deception Island by FT-ICR-MS. Chemosphere 274, 129860. https://doi.org/10.1016/j.chemosphere.2021.129860.

Duarte, B., Matos, A.R., Caçador, I., 2020d. Photobiological and lipidic responses reveal the drought tolerance of Aster tripolium cultivated under severe and moderate drought: Perspectives for arid agriculture in the mediterranean. Plant Physiol. Biochem. 154, 304–315. https://doi.org/10.1016/j.plaphy.2020.06.019.

Duarte, B., Matos, A.R., Marques, J.C., Caçador, I., 2018d. Leaf fatty acid remodeling in the salt-excreting halophytic grass Spartina patens along a salinity gradient. Plant Physiol. Biochem. 124, 112–116. https://doi.org/10.1016/j.plaphy.2018.01.007.

Duarte, B., Matos, A.R., Pedro, S., Marques, J.C., Adão, H., Caçador, I., 2019a. Dwarf eelgrass (Zostera noltii) leaf fatty acid profile during a natural restoration process: Physiological and ecological implications. Ecol. Ind. 106, 105452 https://doi.org/10.1016/j.ecolind.2019.105452.

Duarte, B., Pedro, S., Marques, J.C., Adão, H., Caçador, I., 2017. Zostera noltii development probing using chlorophyll a transient analysis (JIP-test) under field conditions: Integrating physiological insights into a photochemical stress index. Ecol. Ind. 76, 219–229. https://doi.org/10.1016/j.ecolind.2017.01.023.

Duarte, B., Prata, D., Matos, A.R., Cabrita, M.T., Caçador, I., Marques, J.C., Cabral, H.N., Reis-Santos, P., Fonseca, V.F., 2019b. Ecotoxicity of the lipid-lowering drug bezafibrate on the bioenergetics and lipid metabolism of the diatom Phaeodactylum tricornutum. Sci. Total Environ. 650, 2085–2094. https://doi.org/10.1016/j.scitotenv.2018.09.354.

Duarte, B., Santos, D., Caçador, I., 2013. Halophyte anti-oxidant feedback seasonality in two salt marshes with different degrees of metal contamination: search for an efficient biomarker. Funct. Plant Biol. 40, 922. https://doi.org/10.1071/FP12315.

Duarte, I.A., Reis-Santos, P., Novais, S.C., Rato, L.D., Lemos, M.F.L.L., Freitas, A., Pouca, A.S.V., Barbosa, J., Cabral, H.N., Fonseca, V.F., 2020e. Depressed, hypertense and sore: Long-term effects of fluoxetine, propranolol and diclofenac exposure in a top predator fish. Sci. Total Environ. 712 https://doi.org/10.1016/j.scitotenv.2020.136564.

Feijão, E., Cruz de Carvalho, R., Duarte, I.A., Matos, A.R., Cabrita, M.T., Novais, S.C., Lemos, M.F.L., Caçador, I., Marques, J.C., Reis-Santos, P., Fonseca, V.F., Duarte, B., 2020a. Fluoxetine Arrests Growth of the Model Diatom Phaeodactylum tricornutum by Increasing Oxidative Stress and Altering Energetic and Lipid Metabolism. Front. Microbiol. 11, 1803. https://doi.org/10.3389/fmicb.2020.01803.

Feijão, E., Cruz de Carvalho, R., Duarte, I.A., Matos, A.R., Cabrita, M.T., Novais, S.C., Lemos, M.F.L., Caçador, I., Marques, J.C., Reis-Santos, P., Fonseca, V.F., Duarte, B., 2020b. Fluoxetine Arrests Growth of the Model Diatom Phaeodactylum tricornutum by Increasing Oxidative Stress and Altering Energetic and Lipid Metabolism. Front. Microbiol. 11, 1–17. https://doi.org/10.3389/fmicb.2020.01803.

Feijão, E., Franzitta, M., Cabrita, M.T., Caçador, I., Duarte, B., Gameiro, C., Matos, A.R., 2020c. Marine heat waves alter gene expression of key enzymes of membrane and storage lipids metabolism in Phaeodactylum tricornutum. Plant Physiol. Biochem. 156, 357–368. https://doi.org/10.1016/j.plaphy.2020.09.022.

Feijão, E., Gameiro, C., Franzitta, M., Duarte, B., Caçador, I., Cabrita, M.T., Matos, A.R., 2018. Heat wave impacts on the model diatom Phaeodactylum tricornutum: Searching for photochemical and fatty acid biomarkers of thermal stress. Ecol. Ind. 95, 1026–1037. https://doi.org/10.1016/j.ecolind.2017.07.058.

Fonseca, V.F., Duarte, I.A., Duarte, B., Freitas, A., Pouca, A.S.V., Barbosa, J., Gillanders, B.M., Reis-Santos, P., 2021. Environmental risk assessment and bioaccumulation of pharmaceuticals in a large urbanized estuary. Sci. Total Environ. 783, 147021 https://doi.org/10.1016/j.scitotenv.2021.147021.

Fonseca, V.F., Reis-Santos, P., Duarte, B., Cabral, H.N., Caçador, M.I., Vaz, N., Dias, J.M., Pais, M.P., 2020. Roving pharmacies: Modelling the dispersion of pharmaceutical contamination in estuaries. Ecol. Ind. 115, 106437 https://doi.org/10.1016/j.ecolind.2020.106437.

Franzellitti, S., Buratti, S., Du, B., Haddad, S.P., Chambliss, C.K., Brooks, B.W., Fabbri, E., 2015. A multibiomarker approach to explore interactive effects of propranolol and fluoxetine in marine mussels. https://doi.org/10.1016/j.envpol.2015.05.020.

Franzitta, M., Feijão, E., Cabrita, M.T., Gameiro, C., Matos, A.R., Marques, J.C., Goessling, J.W., Reis-Santos, P., Fonseca, V.F., Pretti, C., Caçador, I., Duarte, B., 2020. Toxicity Going Nano: Ionic Versus Engineered Cu Nanoparticles Impacts on the Physiological Fitness of the Model Diatom Phaeodactylum tricornutum. Front. Mar. Sci. 7, 1–18. https://doi.org/10.3389/fmars.2020.539827.

Gameiro, C., Cartaxana, P., Brotas, V., 2007. Environmental drivers of phytoplankton distribution and composition in Tagus Estuary, Portugal. Estuar. Coast. Shelf Sci. 75, 21–34. https://doi.org/10.1016/j.ecss.2007.05.014.

Guillard, R.R., Ryther, J.H., 1962. Studies of marine planktonic diatoms. I. Cyclotella nana Hustedt, and Detonula confervacea (cleve) Gran. Can. J. Microbiol. 8, 229–239. https://doi.org/10.1139/m62-029.

Jónasdóttir, S.H., 2019. Fatty Acid Profiles and Production in Marine Phytoplankton. Mar. Drugs 17, 151. https://doi.org/10.3390/md17030151.

Kumar, M., Kumari, P., Gupta, V., Anisha, P.A., Reddy, C.R.K., Jha, B., 2010. Differential responses to cadmium induced oxidative stress in marine macroalga Ulva lactuca (Ulvales, Chlorophyta). Biometals 23, 315–325. https://doi.org/10.1007/s10534-010-9290-8.

Laureano, G., Figueiredo, J., Cavaco, A.R., Duarte, B., Caçador, I., Malhó, R., Sousa Silva, M., Matos, A.R., Figueiredo, A., 2018. The interplay between membrane lipids and phospholipase A family members in grapevine resistance against Plasmopara viticola. Sci. Rep. 8, 14538. https://doi.org/10.1038/s41598-018-32559-z.

Li, J., Schiavo, S., Rametta, G., Miglietta, M.L., La Ferrara, V., Wu, C., Manzo, S., 2017. Comparative toxicity of nano ZnO and bulk ZnO towards marine algae Tetraselmis suecica and Phaeodactylum tricornutum. Environ. Sci. Pollut. Res. 24, 6543–6553. https://doi.org/10.1007/s11356-016-8343-0.

Liu, J., Dhungana, B., Cobb, G.P., 2018. Environmental behavior, potential phytotoxicity, and accumulation of copper oxide nanoparticles and arsenic in rice plants. Environ. Toxicol. Chem. 37, 11–20. https://doi.org/10.1002/etc.3945.

Lopes, D.G., Duarte, I.A., Antunes, M., Fonseca, V.F., 2020. Effects of antidepressants in the reproduction of aquatic organisms: a meta-analysis. Aquat. Toxicol. 227 https://doi.org/10.1016/j.aquatox.2020.105569.

Matos, A.R., Hourton-Cabassa, C., Ciçek, D., Rezé, N., Arrabaça, J.D., Zachowski, A., Moreau, F., 2007. Alternative oxidase involvement in cold stress response of Arabidopsis thaliana fad2 and FAD3+ cell suspensions altered in membrane lipid composition. Plant Cell Physiol. 48, 856–865. https://doi.org/10.1093/pcp/pcm061.

OECD, 2011. OECD guidelines for the testing of chemicals. Freshwater alga and cyanobacteria, growth inhibition test. Organ. Econ. Coop. Dev. 1–25 https://doi.org/10.1787/9789264203785-en.

Pavlić, Ž., Vidaković-Cifrek, Ž., Puntarić, D., 2005. Toxicity of surfactants to green microalgae Pseudokirchneriella subcapitata and Scenedesmus subspicatus and to marine diatoms Phaeodactylum tricornutum and Skeletonema costatum. Chemosphere 61, 1061–1068. https://doi.org/10.1016/j.chemosphere.2005.03.051.

Pires, V.L., Novais, S.C., Lemos, M.F.L., Fonseca, V.F., Duarte, B., 2021. Evaluation of Multivariate Biomarker Indexes Application in Ecotoxicity Tests with Marine Diatoms Exposed to Emerging Contaminants (preprint). Biology. https://doi.org/10.20944/preprints202103.0735.v1.

Reis-Santos, P., Pais, M., Duarte, B., Caçador, I., Freitas, A., Vila Pouca, A.S., Barbosa, J., Leston, S., Rosa, J., Ramos, F., Cabral, H.N., Gillanders, B.M., Fonseca, V.F., 2018. Screening of human and veterinary pharmaceuticals in estuarine waters: A baseline assessment for the Tejo estuary. Mar. Pollut. Bull. 135, 1079–1084. https://doi.org/10.1016/j.marpolbul.2018.08.036.

Rodrigues, N.M., Batista, J.E., Mariano, P., Fonseca, V., Duarte, B., Silva, S., 2021. Artificial Intelligence Meets Marine Ecotoxicology: Applying Deep Learning to Bio-Optical Data from Marine Diatoms Exposed to Legacy and Emerging Contaminants. Biology 10, 932. https://doi.org/10.3390/biology10090932.

Roma, J., Matos, A.R., Vinagre, C., Duarte, B., 2020. Engineered metal nanoparticles in the marine environment: A review of the effects on marine fauna. Mar. Environ. Res. 161, 105110 https://doi.org/10.1016/j.marenvres.2020.105110.

Silva, M., Feijão, E., da Cruz de Carvalho, R., Duarte, I.A., Matos, A.R., Cabrita, M.T., Barreiro, A., Lemos, M.F.L., Novais, S.C., Marques, J.C., Caçador, I., Reis-Santos, P.,

Fonseca, V.F., Duarte, B., 2020. Comfortably numb: Ecotoxicity of the non-steroidal anti-inflammatory drug ibuprofen on Phaeodactylum tricornutum. Mar. Environ. Res. 161, 105109 https://doi.org/10.1016/j.marenvres.2020.105109.

Taiyun, 2021. taiyun/corrplot.

von Glasow, R., Jickells, T.D., Baklanov, A., Carmichael, G.R., Church, T.M., Gallardo, L., Hughes, C., Kanakidou, M., Liss, P.S., Mee, L., Raine, R., Ramachandran, P., Ramesh, R., Sundseth, K., Tsunogai, U., Uematsu, M., Zhu, T., 2013. Megacities and Large Urban Agglomerations in the Coastal Zone: Interactions Between Atmosphere, Land, and Marine Ecosystems. Ambio 42, 13–28. https://doi.org/10.1007/s13280-012-0343-9.

Wang, L., Zheng, B., 2008. Toxic effects of fluoranthene and copper on marine diatom Phaeodactylum tricornutum. J. Environ. Sci. 20, 1363–1372. https://doi.org/10.1016/S1001-0742(08)62234-2.

Wang, L., Zheng, B., Meng, W., 2008. Photo-induced toxicity of four polycyclic aromatic hydrocarbons, singly and in combination, to the marine diatom Phaeodactylum tricornutum. Ecotoxicol. Environ. Saf. 71, 465–472. https://doi.org/10.1016/j.ecoenv.2007.12.019.

Wang, Y., Zhu, X., Lao, Y., Lv, X., Tao, Y., Huang, B., Wang, J., Zhou, J., Cai, Z., 2016. TiO2 nanoparticles in the marine environment: Physical effects responsible for the toxicity on algae Phaeodactylum tricornutum. Sci. Total Environ. 565, 818–826. https://doi.org/10.1016/j.scitotenv.2016.03.164.

Wickham, H., 2009. In: ggplot2: Elegant Graphics for Data Analysis, Use R!. Springer-Verlag, New York. https://doi.org/10.1007/978-0-387-98141-3.